8-1-2004

Femtosecond Spectrotemporal Magneto-Optics

J.-Y. Bigot
Universite de Strasbourg

L. Guidoni
Universite de Strasbourg

E. Beaurepaire
Universite de Strasbourg

Peter N. Saeta
Harvey Mudd College

Femtosecond Spectrotemporal Magneto-optics

J.-Y. Bigot,* L. Guidoni, E. Beaurepaire, and P. N. Saeta†

Institut de Physique et Chimie des Matériaux de Strasbourg, Unité Mixte CNRS-ULP-ECPM, 23 rue du Loess, B.P. 43, 67034 Strasbourg Cedex, France

(Received 31 October 2003; published 13 August 2004)

A new method to measure and analyze the time and spectrally resolved polarimetric response of magnetic materials is presented. It allows us to study the ultrafast magnetization dynamics of a $CoPt_3$ ferromagnetic film. The analysis of the pump-induced rotation and ellipticity detected by a broad spectrum probe beam shows that magneto-optical signals predominantly reflect the spin dynamics in ferromagnets.

DOI: 10.1103/PhysRevLett.93.077401 PACS numbers: 78.47.+p, 75.40.Gb, 78.20.Ls, 78.66.Bz

During the last few years, femtosecond time-resolved magneto-optics opened the way to measure the magnetization dynamics in ferromagnetic metals on the subpicosecond temporal scale [1,2]. Several experimental configurations have been reported based on the third-order (i.e., pump-probe) magneto-optical (MO) effect [3–12], magnetization-dependent surface second harmonic generation [13–16], and time-resolved two photon photoemission [17,18]. In contrast to the techniques based on photoconductive switches, in which the magnetization dynamics is triggered by a pulsed magnetic field in the picosecond time scale [19–23], a femtosecond temporal resolution can be achieved with MO techniques by inducing the magnetization dynamics via the absorption of an ultrashort laser pulse (the pump pulse). In the case of semiconductors [24] the selection rules on the pump polarization are such that a photogenerated spin population can be created. In the case of metallic ferromagnets, however, the effect of the pump is more subtle, and several questions have been raised about the interpretation of the observed drop in the MO contrast during the first hundreds of femtoseconds following the pump excitation. For example, recent results have shown a discrepancy between the dynamics of differential rotation and ellipticity measured simultaneously with the pump-probe technique [6,9,11]. These observations seem to break the proportionality relationship between the magnetization and Voigt vector, which is the basic assumption of linear magneto-optics. A detailed experimental study of $CoPt_3$ thin films recently demonstrated that this breaking of the commonly admitted interpretation of MO signals occurs during the thermalization time of the electrons following the optical excitation (several tens of femtoseconds) [9]. In particular, in that study it was possible to distinguish between the contributions of the spin and charge populations in the MO signals by carefully separating the dynamics of the diagonal and nondiagonal elements of the time-dependent dielectric tensor. In other studies [25] it has been argued that this discrepancy could originate from a bleaching effect induced by the pump and observed in degenerate pump-probe experiments. In that case, one would expect to observe a spectral signature in the MO response, associated with the population bleaching. The spectral probing of $CoPt_3$ [5] and Fe [11] was previously performed with a probe wavelength at both 800 and 400 nm. In the first case the results did not display significant changes, therefore pleading in favor of the interpretation of the dynamical response in terms of the spin dynamics. Nevertheless, it is clear that to obtain a better understanding of the magnetization dynamics, a spectrotemporal analysis of the MO response is required. In this Letter we describe a reliable method to study the spectrotemporal MO response and to apply it to the case of $CoPt_3$ thin films. This new approach strengthens the idea that femtosecond optical pulses modify the magnetization of ferromagnetic materials.

A consistent spectrotemporal analysis of the MO response can only be obtained using an ellipsometric technique compatible with broad spectra. In this Letter we present such a technique that is based on the spectral detection of the polarimetric signal from the sample placed between crossed polarizers, as a function of the analyzer angle α and pump-probe delay τ compensated for chirp effects. In such a way it is possible to extract from the experimental data both the rotation and the ellipticity obtained in a simultaneous measurement. We used this technique for studying the spectral and temporal dependence of the MO contrast in a $CoPt_3$ sample. The results show that a slight spectral dependence is present in the static MO response as already demonstrated in previous studies [26,27]. On the contrary, the dynamical behavior of the relative variations of rotation and ellipticity are identical and do not show any spectral dependency. Our interpretation of these results is that in a $CoPt_3$ alloy the spin dynamics dominates the MO contrast in the visible part of the spectrum. This study corroborates the fact that a femtosecond optical control of correlated spin phases is now achievable.

The samples are thin films (thickness of 21.5 nm) of $CoPt_3$ alloy grown on a (0001) oriented sapphire crystal as described in Ref. [9]. Laser pulses of 150 fs duration are delivered at a repetition rate of 5 kHz by a Ti:sapphire

regenerative amplifier operating at a central wavelength of 790 nm. Part of the energy is used to generate the pump beam at 400 nm (200 fs, the maximum fluence on the sample is 1 mJ/cm^2) by second harmonic generation in a 1.5 mm thick beta barium borate crystal. Another part of the energy (less than 1 μJ) is focused on a (0001) oriented sapphire crystal (thickness 2 mm) to generate a supercontinuum whose spectrum spreads from 480 to 750 nm. Most of the chirp compensation of the continuum is obtained by a double pass prisms compressor. The residual group velocity dispersion has been characterized by two photon absorption in a thin semiconductor crystal with a large band gap (ZnS). It is of the order of 850 fs in the entire spectral range and less than 150 fs in the range 500–650 nm. This residual chirp is deconvoluted from the spectrotemporal MO signals by an appropriate conform transformation in the (λ, τ) plane [28]. The detection scheme that we adopted to obtain the time and spectrally resolved MO signals is sketched in Fig. 1. The p-polarized probe beam is focused on the sample in spatial overlap with the pump by a 150 mm focal length spherical mirror. Both the transmitted and the reflected probes pass through Glan polarizers oriented at an angle $\pi/2 + \alpha$ with respect to the initial probe polarization. The angles α_F and α_K (for the transmitted and reflected beams, respectively) can be varied by two rotation stages with a precision of ± 0.3 mrad. The analyzed beams are then focused on the entrance slit of an imaging spectrometer, and their spectral intensity is recorded by a nitrogen-cooled charge-coupled device detector as a function of the analyzer angle α. Alternatively, temporal cross sections at a given wavelength can be obtained by spectral selection (FWHM of 15 nm) of the probe beam. The analyzed beams are then measured with two photomultipliers using a lock-in detection scheme. In both cases the static polarimetric signals and their pump-induced variations (as a function of τ) are acquired for the two opposite remnant magnetization states of the sample.

Let us now consider the expression of the intensity $I_\pm$ that impinges on the photodetectors in the polarimetric configuration described above for two opposite magnetization states $\pm M$ of the sample. The polarimetric configuration is a simplified version of a rotating analyzer ellipsometer. An elementary analysis using Jones matrices [29] in the small angle limit leads to

$$I_{\pm M} = I_0[\alpha^2 - 2\alpha(\theta_0 \pm \theta_M) + (\theta_0^2 + \eta_0^2 + \theta_M^2 + \eta_M^2) \pm 2(\theta_0\theta_M + \eta_0\eta_M)], \quad (1)$$

where I_0 is the intensity measured with the analyzer parallel to the polarizer; α is the analyzer angle (with respect to the crossed orientation); θ_0 and η_0 are the nonmagnetic rotation and ellipticity induced by the sample; and θ_M and η_M are the MO rotation and ellipticity (that change sign when M is reversed). The quantities θ_0, θ_M, η_0, η_M, and I_0 are all wavelength dependent. As already underlined by Koopmans [2], for a fixed detection angle α and in the absence of further analysis this method of detection is not very powerful because it mixes the contributions of MO rotation and ellipticity. On the other hand, reliable information can be obtained performing the experiment as a function of the parameter α. In particular, by fitting simultaneously the experimental data obtained for two opposite magnetization directions, it is possible to separate the different contributions and to measure both θ_M and η_M. An example of this analysis is given in Fig. 2 in which the data obtained in a static spectrally resolved experiment are displayed. At a given wavelength [$\lambda = 710$ nm in the example reported in Figs. 2(a) and 2(c)], a couple of parabolas corresponding

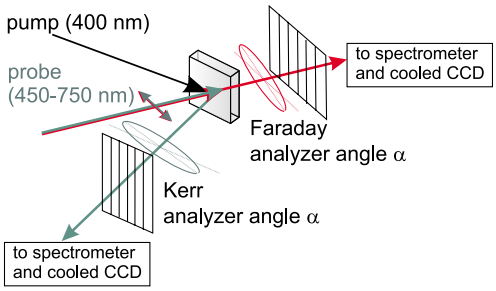

FIG. 1 (color online). Polarimetric detection scheme based on the rotating analyzer ellipsometer.

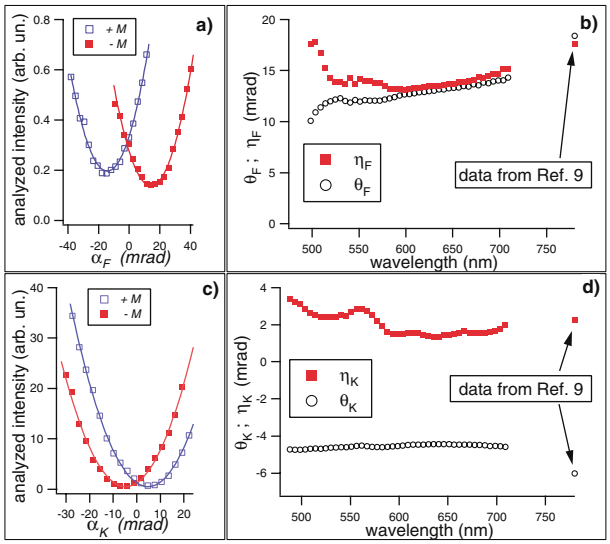

FIG. 2 (color online). Probe intensity ($\lambda = 710$ nm) as a function of the analyzer angle α in the Faraday (a) and Kerr (c) configurations. The open and filled symbols correspond to two opposite remnant magnetizations. The continuous lines are the fits according to Eq. (1). The spectral dependences of the static Faraday (b) and Kerr (d) MO angles θ and η are obtained with the same fitting procedure for each wavelength. For comparison we report the ellipticity and rotation measured with the photoelastic modulator technique at $\lambda = 790$ nm [9].

to the two opposite magnetization directions is obtained both for the Kerr and for the Faraday geometry. The continuous lines correspond to the fit obtained according to the Eq. (1). This same procedure performed for each wavelength allows us to retrieve the spectral dependence of θ_M and η_M for the Faraday [Fig. 2(b)] and for the Kerr [Fig. 2(d)] geometry. These results, obtained in a CoPt alloy grown by molecular beam epitaxy on a sapphire substrate, are consistent with previous measurements on other CoPt alloys [26,27]. For comparison we also report in Fig. 2 the static values of θ_M and η_M measured on the same sample at $\lambda = 790$ nm (with a $\simeq 40$ nm bandwidth) in a previous experiment made with 20 fs time resolution [9].

This technique becomes very powerful when determining the dynamical behavior of the MO contrast. In the case of a pump-probe experiment the same kind of analysis still holds, but the shape and position of the parabolas will evolve as a function of τ because some of the parameters in Eq. (1) are time dependent. Indeed, one expects temporal contributions from I_0 (differential reflectivity and transmission) and, more importantly, from θ_M and η_M. The parameters θ_0 and η_0 are not expected to be dependent on τ as long as one is not interested in coherent phenomena that appear only during the pump-probe temporal overlap. A first straightforward analysis of the time-dependent data can be obtained by noticing that the quantity R, defined as

$$R = \frac{I_{+M}(\tau) - I_{-M}(\tau)}{4I_0(\tau)} = -\theta_M(\tau)\alpha + \theta_M(\tau)\theta_0 + \eta_M(\tau)\eta_0, \qquad (2)$$

has a linear behavior with respect to α with a slope $\theta_M(\tau)$. This behavior is, indeed, observed in Fig. 3(a) where the results, obtained for the Faraday configuration, are displayed. Figure 3(b) displays the variation of $R(\tau)$ with respect to the static R. In these measurements the probe is spectrally integrated in the range $\lambda =$ 500–700 nm. Even more interesting is the fact that all the lines in Fig. 3 cross the abscissa $R = 0$ at the same point. According to the relation (2) this behavior is possible if and only if the relative variations of the rotation and ellipticity are strictly identical, i.e., $\frac{\Delta\theta_M}{\theta_M}(\tau) \equiv \frac{\Delta\eta_M}{\eta_M}(\tau)$. We obtained another confirmation of this result by a different analysis of the same experimental data set. The procedure consists in fitting simultaneously a set of four parabolas for each delay τ: the two static parabolas and the two time-dependent parabolas. The number of free parameters in this fit is dramatically reduced by the fact that the parabolas share the same static parameters and that the time dependence of the parameter I_0 is obtained by an independent measurement of the differential transmission and reflectivity. In Figs. 4(a) and 4(b) we show an example of this analysis for a pump-probe delay $\tau = +600$ fs. Both in the Faraday and Kerr configurations, the experimental results are well described by a set of parameters in which $\frac{\Delta\theta_M}{\theta_M}(\tau) \equiv \frac{\Delta\eta_M}{\eta_M}(\tau)$. Moreover the time evolution of the MO contrast obtained in Kerr and Faraday geometries display the same time evolution within the experimental error [Fig. 4(c)].

Let us now focus on the spectral dependence of the MO dynamical behavior. A current understanding of the ultrafast demagnetization dynamics in transition metals is that it is due to time-dependent electronic and spin temperatures. Such interpretation suggests that no spectral dependence should be observed in the relative change

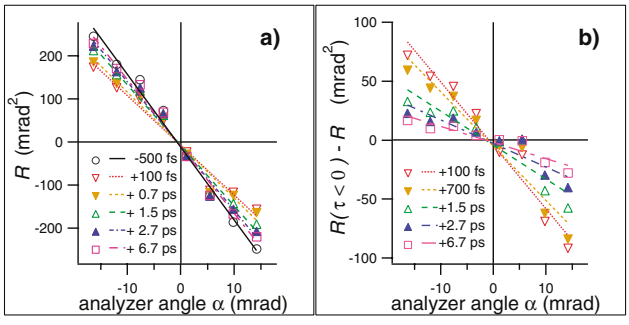

FIG. 3 (color online). (a) $R(\alpha)$ as defined in Eq. (2) for different delays τ. For clarity in (b) we show $R(\tau < 0) - R(\tau)$.

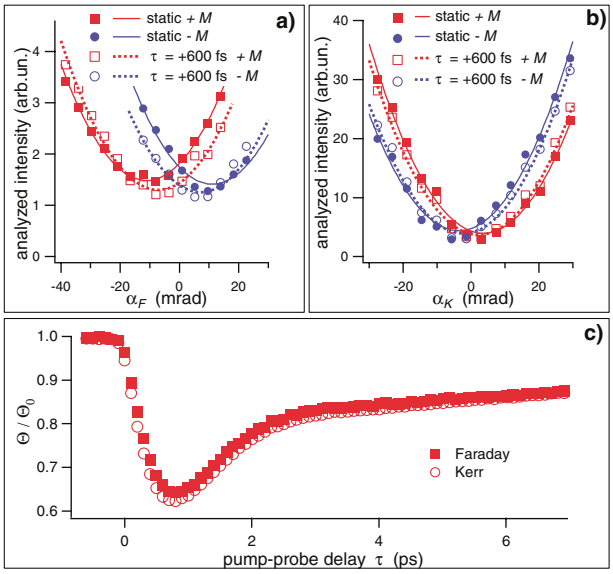

FIG. 4 (color online). Probe intensity as a function of the analyzer angle α in the Faraday (a) and Kerr (b) configurations (same condition as in Fig. 3). The filled squares (circles) correspond to a $+M$ ($-M$) remnant magnetization measured for a negative delay (static contribution). Open symbols: $\tau = +600$ fs. Continuous and dotted lines: cumulative fit of the four parabolas with Eq. (1). In these fits θ_0, η_0 are blocked, I_0 evolves according to the differential transmission (or reflectivity) data, and θ_M, and η_M parameters are constraints such that $\frac{\Delta\theta_M}{\theta_M}(\tau) \equiv \frac{\Delta\eta_M}{\eta_M}(\tau)$. (c) Corresponding time evolution of the rotations Θ (Kerr and Faraday geometries).

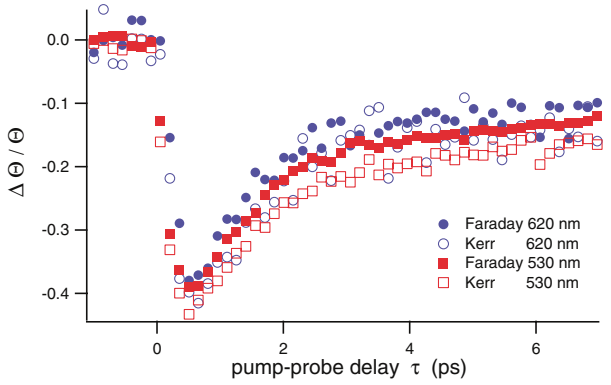

FIG. 5 (color online). Relative variations of the rotation $\Delta\Theta/\Theta$ measured at 530 nm (squares) and 620 nm (circles) in the Kerr (empty symbols) and Faraday (filled symbols) configurations.

$\Delta M/M = \frac{\Delta(n_\uparrow - n_\downarrow)}{n_\uparrow - n_\downarrow}$ ($n_\uparrow$ and $n_\downarrow$ being the majority and minority spins) neither as a function of the pump frequency nor as a function of the probe frequency. As long as the time-resolved MO signals are dominated by the magnetization dynamics, a flat spectral response should be observed for the temporally dependent relative variations of the MO rotation and ellipticity even in the presence of a spectral dependence of the corresponding static quantities. To investigate this assumption we measured the dynamics of the differential rotation $\Delta\theta_M/\theta_M$ at several wavelengths (spectral selection of the continuum probe with a FWHM of 15 nm) both in Kerr and Faraday geometry. The observed dynamics of the MO contrast does not depend on the wavelength of detection. As an example we display in Fig. 5 the temporal cross sections of $\Delta\theta_M/\theta_M$ centered at 530 and 620 nm.

In conclusion, we demonstrated that the rotating analyzer ellipsometry is an appropriate experimental configuration to measure the spectrally and time-resolved MO contrast. Our results prove that the laser-induced dynamics of the MO contrast in a CoPt alloy does not depend on the probe wavelength. In particular, in the whole spectral range that we explored ($\lambda = 480$–700 nm) we found that $\frac{\Delta\theta_M}{\theta_M}(\tau) \equiv \frac{\Delta\eta_M}{\eta_M}(\tau)$. Additional measurements obtained with a spectral selection of the probe wavelength confirm that the dynamical behavior of the MO contrast is geometry (Kerr or Faraday) and wavelength independent. These results corroborate the fact that time-resolved magneto-optics gives access to the genuine magnetization dynamics and that a femtosecond laser pulse can change the ferromagnetic order of a metal in the subpicosecond regime.

P. S. acknowledges financial support from CNRS.

*Electronic address: Jean-Yves.Bigot@ipcms.u-strasbg.fr
†Permanent address: Harvey Mudd College, Claremont, CA 91711, USA.

[1] J.-Y. Bigot, E. Beaurepaire, L. Guidoni, and J.-C. Merle, in *Magnetism: Molecules to Materials III. Nanosized Magnetic Materials*, edited by J. S. Miller and M. Drillon (Wiley-VCH, Weinheim, Germany, 2001), pp. 355–384.
[2] T. Rasing, H. van den Berg, T. Gerrits, and J. Hohlfeld, in *Spin Dynamics in Confined Magnetic Structures II*, edited by B. Hillebrands and K. Ounadjela (Springer-Verlag, Berlin, Heidelberg, 2003), pp. 213–251; B. Koopmans, *ibid.*, pp. 253–316.
[3] E. Beaurepaire, J.-C. Merle, A. Daunois, and J.-Y. Bigot, Phys. Rev. Lett. **76**, 4250 (1996).
[4] G. Ju *et al.*, Phys. Rev. B **57**, R700 (1998).
[5] E. Beaurepaire *et al.*, Phys. Rev. B **58**, 12 134 (1998).
[6] B. Koopmans, M. van Kampen, J. T. Kohlhepp, and W. J. M. de Jonge, Phys. Rev. Lett. **85**, 844 (2000).
[7] T. Kise *et al.*, Phys. Rev. Lett. **85**, 1986 (2000).
[8] J. Hohlfeld *et al.*, Phys. Rev. B **65**, 012413 (2002).
[9] L. Guidoni, E. Beaurepaire, and J.-Y. Bigot, Phys. Rev. Lett. **89**, 017401 (2002).
[10] M. van Kampen *et al.*, Phys. Rev. Lett. **88**, 227201 (2002).
[11] T. Kampfrath *et al.*, Phys. Rev. B **65**, 104429 (2002).
[12] R. Wilks, N. D. Hughes, and R. J. Hicken, J. Appl. Phys. **91**, 8670 (2002).
[13] J. Hohlfeld, E. Matthias, R. Knorren, and K. H. Bennemann, Phys. Rev. Lett. **78**, 4861 (1997).
[14] J. Güdde *et al.*, Phys. Rev. B **59**, R6608 (1999).
[15] H. Regensburger, R. Vollmer, and J. Kirschner, Phys. Rev. B **61**, 14716 (2000).
[16] A. V. Melnikov, J. Güdde, and E. Matthias, Appl. Phys. B **74**, 735 (2002).
[17] A. Scholl, L. Baumgarten, R. Jacquemin, and W. Eberhardt, Phys. Rev. Lett. **79**, 5146 (1997).
[18] H.-S. Rhie, H. A. Dürr, and W. Eberhardt, Phys. Rev. Lett. **90**, 247201 (2003).
[19] A. Y. Elezzabi, M. R. Freeman, and M. Johnson, Phys. Rev. Lett. **77**, 3220 (1996).
[20] B. C. Choi *et al.*, Phys. Rev. Lett. **86**, 728 (2001).
[21] T. Gerrits *et al.*, Nature (London) **418**, 509 (2002).
[22] H. W. Schumacher *et al.*, Phys. Rev. Lett. **90**, 017204 (2003).
[23] J. P. Park *et al.*, Phys. Rev. B **67**, 020403(R) (2003).
[24] J. A. Gupta, R. Knobel, N. Samarth, and D. D. Awschalom, Science **292**, 2458 (2001).
[25] B. Koopmans, M. van Kampen, and W. J. M. de Jonge, J. Phys. Condens. Matter **15**, S723 (2003).
[26] R. J. Lange *et al.*, Phys. Rev. B **58**, 351 (1998).
[27] L. Uba *et al.*, Phys. Rev. B **64**, 125105 (2001).
[28] S. A. Kovalenko, A. L. Dobryakov, J. Ruthmann, and N. P. Ernsting, Phys. Rev. A **59**, 2369 (1999).
[29] R. M. A. Azzam and N. Bashara, *Ellipsometry and Polarized Light* (North-Holland, Amsterdam, 1977).